ASIAN JOURNAL OF AGRICULTURE
Volume 10, Number 1, June 2026
Pages: 9

E-ISSN: 2580-4537
https://doi.org/10.13057/asianjagric/g100125

Characterization of acid-modified corn cob biochar for potential alkaline soil remediation

MAHMOUD A. M. HASSAN[1], MOHAMED E. A. EL-SAYED[1,♥], MOHAMED H. ABDALLAH[2], AHMED A. GAHLAN[2]

[1]Soils, Water and Environment Research Institute, Agriculture Research Center. Giza 12112, Egypt. Tel.: +20-2-01224063877,
♥email: eid1592003@yahoo.com
[2]Department of Chemistry, Faculty of Science, Al-Azhar University. Assiut 71524, Egypt

Manuscript received: 11 October 2025. Revision accepted: 10 February 2026.

Abstract. *Hassan MAM, El-Sayed MEA, Abdallah MH, Gahlan AA. 2026. Characterization of acid-modified corn cob biochar for potential alkaline soil remediation. Asian J Agric 10 (1): g100125. https://doi.org/10.13057/asianjagric/g100125.* Biochar (BC), derived from agricultural residues, is increasingly recognized for its capacity to enhance soil quality and contribute to the reduction of greenhouse gas emissions. Conversely, the typically high pH of BC limits its effectiveness in alkaline soils, such as those prevalent in Egypt. In order to overcome this difficulty, this study produced BC from corncobs via slow pyrolysis at 350°C for an hour at a heating rate of 10°C min^{-1}. Its surface was modified with phosphoric acid, sulfuric acid, and humic acid, resulting in PBC, SBC, and HBC, respectively. Biochar and its modified forms were characterized by elemental analysis, Fourier Transform Infrared (FTIR) spectroscopy, X-Ray Diffraction (XRD), Brunauer-Emmett-Teller (BET) surface area, and Field-Emission Scanning Electron Microscopy (FE-SEM). The findings revealed that the pH of MBCs has decreased from 7.87 to 7.13 compared to 8.32 for BC. This adjustment can improve the compatibility of BC with alkaline soils. In addition, all Modified Biochars (MBCs) have higher surface areas of 83.73, 79.60, and 75.23 m^2/g for HBC, SBC, and PBC, respectively, compared to 73.41 m^2/g for unmodified BC. Pores of MBCs were microporous, while BC is composed of mesopores. The elemental analysis demonstrated that the MBCs have more functional groups than BC, which improves BC properties and applications. Overall, the MBCs demonstrated enhanced specific physicochemical properties, particularly in pH adjustment, functional groups, surface areas, and pore size distribution following the order: HBC>SBC>PBC>BC, suggesting their potential as effective ameliorants for alkaline soils. These results highlight the benefits of agricultural waste and tailoring BC properties to address the specific needs of alkaline soils, while also contributing incidentally to carbon sequestration as a beneficial secondary outcome.

Keywords: Acid modification, alkaline soil, biochar, corncobs, slow pyrolysis

INTRODUCTION

Today, the world faces significant social, economic, and environmental challenges, including climate change, energy scarcity, soil degradation from nutrient loss, and limited freshwater resources, particularly in arid and semi-arid regions such as Egypt (Jubori and Kaynak 2025). To sustain agricultural productivity, the use of low-quality irrigation water, such as saline water, has become increasingly necessary. However, saline irrigation often leads to soil salinity and sodicity buildup, which degrade soil structure, reduce infiltration, and impair crop performance (Zhang et al. 2024). Where approximately 900,000 hectares of Egypt's irrigated land are affected by salinity, leading to substantial yield reductions when saline water is used for irrigation (Tessema et al. 2022; Otaibi et al. 2024). Consequently, soil salinity remains a major constraint to soil fertility, water use efficiency, and sustainable agricultural development (Hammam and Mohamed 2020).

The inappropriate burning (often through open burning) of agricultural residues such as rice straw, corncobs, and maize stalks poses environmental challenge (Ashour and Belal 2020). Pyrolysis in an oxygen-limited environment (slow at 300-700°C and fast at 550-1000°C) provides a sustainable way to turn these leftovers into biochar (BC) (Phares et al. 2020; Tenic et al. 2020). BC, a porous substance rich in carbon, not only enhances soil fertility and structure but also helps mitigate salinity by adsorbing soluble salts, reducing exchangeable sodium, and improving water retention, thereby alleviating salt stress and supporting sustainable agriculture (El-Naggar et al. 2019; Wu et al. 2024). BC is usually alkaline with a pH ranging from 7 to 10, which makes it beneficial for improving acidic soils by enhancing nutrient availability. Unfortunately, most Egyptian agricultural soils are neutral to alkaline (pH 7-8.5) because of salt accumulation from saline irrigation and poor drainage, which reduces the immediate benefits of BC. The physicochemical properties of BC, such as surface area, pore structure, and functional groups, depend on its feedstock type and production conditions, which can restrict its effectiveness. To overcome this limitation, post-production modification techniques, particularly acid modification, have been employed to increase surface acidity and add oxygenated functional groups, decreasing the pH of BC, making MBCs more suitable for improving alkaline soils and wider environmental applications (Ippolito et al. 2020).

Despite progress in biochar research, limited studies have systematically compared different acid modification techniques for BC derived from local agricultural wastes like corncobs, especially under the alkaline soil conditions common in arid regions like Egypt. Most research has focused on single modification agents or general adsorption improvements without considering high soil pH and salinity challenges (Joshi et al. 2023).

The acid treatments with sulfuric, phosphoric, or Humic Acid (HA) can significantly enhance BC's physicochemical and agronomic properties. Phosphoric acid modification, commonly used, enriches BC with phosphate groups, improving nutrient availability such as phosphorus, potassium, and micronutrients, while HA modifies BC's surface chemistry, increasing microbial activity and soil enzyme functions, which may synergistically enhance soil fertility and plant growth. Overall, acid modifications of BC with these acids improve its nutrient content, soil interaction, and environmental remediation capacities by altering surface functional groups and bioavailability of nutrients (Hammerschmiedt et al. 2021; Alhawas et al. 2023; Kopp et al. 2024).

This study aims to fill this gap by preparing corncob-based BC and modifying its surface using various acids (humic acid, sulfuric acid, and phosphoric acid) to overcome its limitations for future applications in alkaline soils, thereby offering a sustainable pathway for agricultural waste valorization and improved soil management in alkaline environments (Tomczyk et al. 2020). Consequently, the following research questions are addressed in this study: (i) How do different acid modifications alter the physicochemical properties of corncob-derived BC to overcome its inherent limitations for future applications in alkaline soils? and (ii) Which modified BC, based on its modified physicochemical properties, is best suited to be advanced to future incubation and field studies for alkaline soil amendment?

To answer these questions, the research aims to: (i) produce and characterize unmodified and acid-modified biochars; (ii) thoroughly evaluate and compare the resulting acid-modified biochar's physicochemical features; and (iii) Relate these characteristics to their potential relevance in improving alkaline soil conditions in future applications. Hence, this research offers new insights into the thorough characterization, evaluation, and systematic comparison of three different acid modifications applied to BC derived from a locally available agricultural waste material. It also explicitly links the physicochemical improvements that result from these acid modifications to their potential use as soil amendments for alkaline soils in a subsequent experimental phase.

MATERIALS AND METHODS

Corncob biomass

Corncob samples were collected from an experimental farm at the shandwell agricultural research station, sohag governorate, egypt. After air drying in the sun for one week to remove moisture, the samples were crushed and ground to pass through a 2 mm sieve. The powders were then washed with deionized water to remove potential contaminants and dried at 70±3°C until a constant weight was achieved (Figure 1). Then, it was stored in covered porcelain dishes.

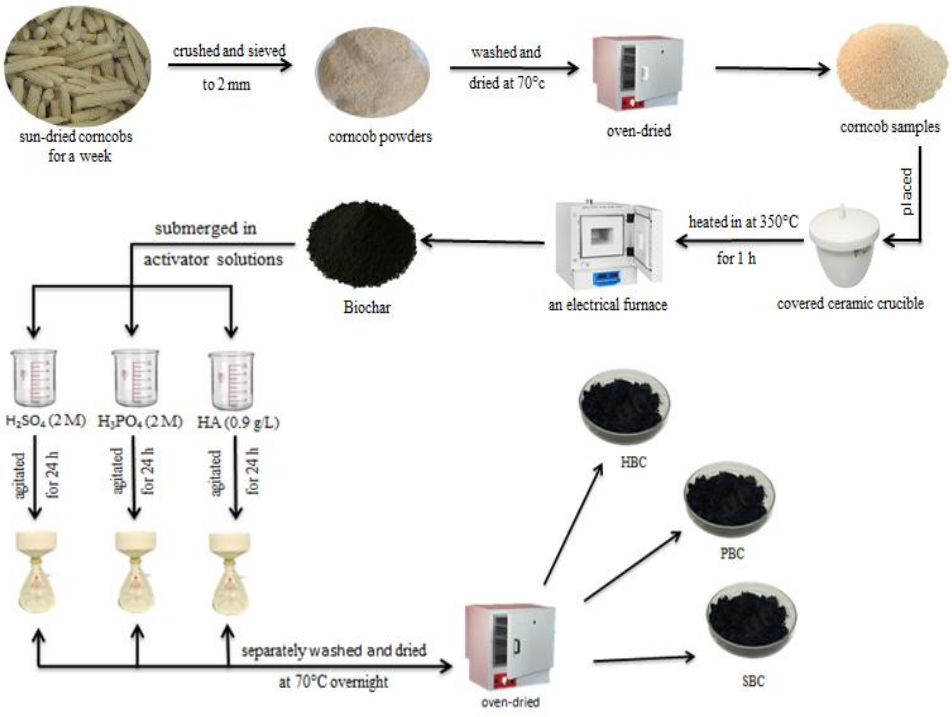

Figure 1. Schematic illustration of the biochar and modified biochars' preparation

Preparation of biochar

To prepare BC, corncob samples were placed in a covered ceramic crucible and heated in an electrical furnace at 350°C for 1 hour, with a heating rate of 10°C /min under oxygen-limited conditions, to obtain the initial BC (Figure 1) (Reza et al. 2020; El-Sayed et al. 2021). This temperature was chosen for BC production to preserve functional groups (e.g., carboxyl and hydroxyl) and inhibit pH elevation to improve soil fertility, as indicated in references (El-Sayed et al. 2021; Yuanbo et al. 2025). The yield of BC was then determined by weighing the crucible as in equation 1.

$$\text{BC yield (\%)} = (m_1 / m_0) \times 100\% \quad [1]$$

Where m_0 (g) is the dry weight of corncob samples before pyrolysis, and m_1 (g) is the weight of BC after charring. The BC yield was 53%. After that, these BC samples were sealed and kept for later use.

A specific amount of BC was placed in a ceramic crucible at 105°C in an electrical furnace, and the weight was recorded after a constant value was reached. This made it possible to determine the moisture content using equation 2, which is based on mass loss.

$$\text{Moisture content (\%)} = (m_0 - m_1) / m_0 \times 100\% \quad [2]$$

Where m_0 (g) represented the weight of the BC before to its entry into an electrical furnace, and m_1 (g) represented the weight of the BC following drying.

A specific quantity of BC was placed in a ceramic crucible, charred at 800°C in an electrical furnace, and the weight was recorded once a consistent value was achieved in order to determine the ash content as in equation 3.

$$\text{Ash content (\%)} = (m_1 / m_0) \times 100\% \quad [3]$$

Where m_0 (g) was the BC dry weight before charring, and m_1 (g) was the BC weight after charring.

The Debye-Scherrer equation in equation 4 was used to determine the average particle size (D) of BC (El-Sayed et al. 2018).

$$D = K\lambda / \beta\cos\theta \quad [4]$$

Where λ, β, and θ stand for the X-ray wavelength light, the diffraction angle, and the whole breadth of the half maximum of the diffraction peak, respectively. The form factor K is often considered to be 0.89.

The pH and EC were measured in the lab by means of combined digital pH and EC meter, respectively. All measurements of pH, EC, moisture content, and ash content were performed in triplicate to ensure analytical accuracy. Scanning Electron Microscopy (SEM), FT-IR spectra, elemental analysis, X-Ray Diffraction (XRD), and BET surface area were used to characterize BC (Assirey and Altamimi 2021).

Humic Acid (HA)

According to Swift (1996), humate salt (Sigma-Aldrich Co., Germany) is used to prepare HA. HA is precipitated by dissolving humate salt in distillate water with potassium hydroxide (5 M) and adjusting the pH to 2 with HCl. The precipitated HA was redissolved again in 0.5 M potassium hydroxide, and the pH was also adjusted to 2 by adding HCl. This dissolution and precipitation were repeated three times to ensure the purification of the HA from other metals, such as silicate, aluminum and iron. FT-IR and elemental analysis were used to describe HA, with elemental analysis being one of the most straightforward and significant methods of HA characterization (Bai et al. 2024). The HA's elemental analysis results for the percentages of carbon, hydrogen, nitrogen, sulfur, and oxygen were 40.06, 4.57, 0.79, 0.73, and 53.83, respectively.

Preparation of biochar and humic acid stock solutions

For the adsorption experiment, the stock solutions of BC suspensions (30 g/ L) were set at pH 6 and KCl (0.01 M). In a 250 mL beaker, distilled water and HA powder were combined. To improve the solid-state HA's dissolution, a few drops of KOH (0.05 M) were added while stirring. The pH was then adjusted to 6 by adding potassium hydroxide or hydrochloric acid, and the ionic strength of HA solutions was adjusted to 0.01 M by adding KCl salt. The concentration of HA in the stock solution was 1.5 g / L. At 4±0.1°C, the prepared solution was kept.

Humic acid adsorption on biochar

Batch adsorption experiments were conducted by mixing 30 g/L of BC with varying HA concentrations (0.125 to 1 g/L) in an orbital shaker at 500 rpm for 24 hours (pH 6, ionic strength 0.01 mol dm^{-3} KCl) in order to reach equilibrium. A UV spectrophotometer was used to determine the amount of unadsorbed HA in each sample supernatant (Bai et al. 2024). The results were reported using the average of the triplicate trials.

Equation 5 is used to express the adsorption capacity, q_e (mg/g) (El-Sayed et al. 2018):

$$q_e = V (C_0 - C_e) / m \quad [5]$$

Where C_o and C_e (mg/L) are the initial and equilibrium HA concentrations, V (L) is an aqueous solution containing HA volume, and m (g) is the BC weight. The results were reported using the average of the triplicate trials.

Experimental data is often fitted and interpreted using equations from the Freundlich and Langmuir models. The heterogeneity surface is described by the Freundlich equation; the n value represents the degree of nonlinearity between adsorption and solution concentration, and monolayer coverage on a homogenous surface with similar adsorption sites is assumed by the Langmuir isotherm (Elkony et al. 2020).

Equation 6 displays the Freundlich isotherm equation in its linear version, which was utilized to simulate the equilibrium data:

$$\text{Log } q_e = \text{Log } K_f + (1 / n) \text{ Log } C_e \quad [6]$$

Where n is the adsorption strength and k_f $(mg/g)(mg/L)^{1/n}$ is the Freundlich parameter. Plotting log q_e vs log C_e allowed for the determination of both k_f and n parameters.

Equation 7 below provides a mathematical expression of the Langmuir isotherm in linear form, which is used to simulate the equilibrium data:

$$C_e / q_e = 1 / (q_m K_L) + C_e / q_m \quad [7]$$

Where q_m (mg/g) is the monolayer adsorption capacity, K_L (L/g) is the Langmuir constant, C_e (mg/L) is the equilibrium concentration of HA in solution, and q_e (mg/g) is the concentration of HA on the surface. Plotting C_e/q_e

versus C_e allowed for the determination of both q_m and K_L parameters, define the adsorption isotherm.

Preparation of humic acid-modified biochar, H_3PO_4-modified biochar, and H_2SO_4-modified biochar

The humic acid-modified BC, H_3PO_4-modified BC, and H_2SO_4-modified BC, designated HBC, PBC, and SBC, respectively, were prepared separately using three different acids: HA, H_3PO_4, and H_2SO_4, respectively, through different chemical mechanisms. HA (a complex organic acid) for surface functionalization, whereas H_3PO_4 and H_2SO_4 (strong mineral acids) for chemical activation and surface etching as shown in Figure 1. First, for preparation of HBC, 30 g of BC were submerged in 1 L of HA solution at a concentration of 0.9 g/L, based on the adsorption experiment conducted in this study to yield optimal modification efficiency. Second, for PBC preparation, 30 g of BC were submerged in 294 mL of H_3PO_4 (2 M), equivalent to a solid-to-liquid (w/v) ratio of 1:9.8 and corresponding to a 1:1.92 mass ratio of BC to pure acid in accordance with the phosphoric acid treatment methodology described by Dechapanya and Khamwichit (2023). Third, for SBC preparation, 30 g of BC were submerged in 281.4 mL of H_2SO_4 (2 M), equivalent to a solid-to-liquid (w/v) ratio of 1:9.38 and corresponding to a 1:1.84 mass ratio of BC to pure acid, in agreement with the method reported by Wang et al. (2023). All mixtures were agitated at 500 rpm for 24 hours at 25±2°C. Subsequently, the MBCs samples were separated using a Büchner funnel with Whatman no. 1 filter paper and washed with distilled water about 3-4 times until the pH of the wash water remained constant (pH~7). Then, it was oven-dried overnight at 70±3°C after discarding the supernatants, and it was stored in sealed containers until use (El-Sayed et al. 2018). The moisture content and ash content of MBCs was calculated in the same way as last described. The pH and EC were also measured in the lab in the same way as last described. All measurements of pH, EC, moisture content, and ash content were performed in triplicate to ensure analytical accuracy. The MBCs were also characterized by elemental analysis, X-Ray Diffraction (XRD), FT-IR spectra, Scanning Electron Microscopy (SEM), and BET surface area.

Characterization of biochar and modified biochars

The contents of C, H, N, and S were determined using a CHNS elemental analyzer. The oxygen contents were calculated by difference. The surface functional groups of BC and MBCs were determined using Fourier Transform Infrared Spectroscopy (FT-IR) spectra over 450-4,000 cm^{-1}, and peaks were compared. The crystalline structure was characterized using X-Ray Diffraction (XRD). The specific surface area, pore volume, and pore diameter were obtained from N_2 adsorption-desorption isotherms at 77 K using the BET method. Additionally, the surface morphology of BC and MBCs was observed using Scanning Electron Microscopy (SEM).

Data processing and statistical analysis

Microsoft Excel 2019 was used to arrange and tabulate all experimental data and computed values. OriginPro 8 was used for the processing and graphical representation of FTIR, XRD, and adsorption isotherm (Langmuir and Freundlich) data. These tools were used to ensure accurate data computation, visualization, and presentation.

Statistical analysis was performed using SPSS Statistics version 26. All measurements were conducted in triplicate (n=3). To determine significant differences among sample means, a one-way Analysis of Variance (ANOVA) was applied, followed by Duncan's Multiple Range test for post-hoc comparisons. The significance level was set at $\alpha = 0.05$. Results are presented as mean ± standard deviation (SD), with different superscript letters indicating statistically significant differences ($p < 0.05$).

RESULTS AND DISCUSSION

Humic acid adsorption on biochar

In order to assess the distribution of HA on the BC surface during the adsorption process, it was crucial to fit the adsorption data. Complete HA coverage on BC could be achieved with 0.9 g/L HA, according to adsorption isotherm data (Figure 2). This exact concentration was used to prepare HBC.

Table 1 lists the intercept and slope parameters that were obtained from the Freundlich and Langmuir isotherm plots, both of which showed strong linear fits. A value of 1.71703 was found for n in the Freundlich isotherm, indicating favorable adsorption and falling between 1 and 10. The Langmuir isotherm, however, offered the greatest match to the experimental data according to the coefficient of correlation (R^2) values, (R^2=0.9968). Additionally, 63.29 mg/g was determined to be the maximal monolayer adsorption capacity (q_m) using the Langmuir equation.

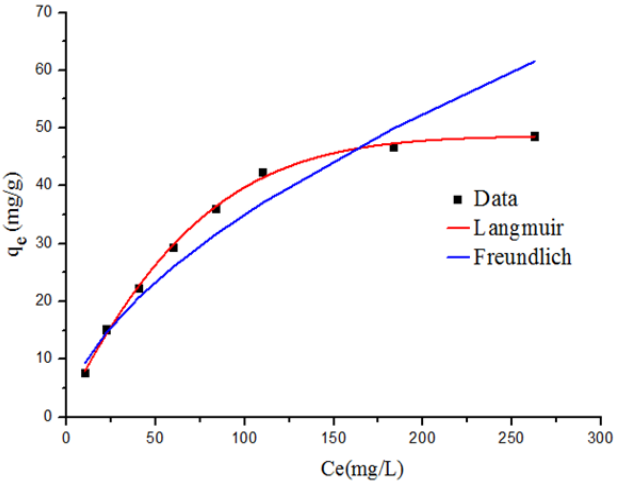

Figure 2. Adsorption isotherm for HA adsorption onto BC by fitting the Langmuir and Freundlich isotherm models at 25±2°C, pH 6, ionic strength 0.01 mol dm^{-3} KCl, initial HA concentration range = 0.125 to 1 g L^{-1}, and shaking rate = 500 rpm for 24 hours. The data points were the average of triplicates

Table 1. Comparisons between Freundlich and Langmuir adsorption isotherm constants for HA onto BC at 25±2°C, pH 6, ionic strength 0.01 mol dm^{-3} KCl, initial HA concentration range = 0.125 to 1 g L^{-1}, and shaking rate = 500 rpm for 24 hours

Adsorbent	Langmuir			Freundlich		
	q_m (mg g^{-1})	K_L (L mg^{-1})	R^2	n	K_f (mg/g) $(mg/L)^{1/n}$	R^2
BC	63.29 ± 4.16	0.01452 ± 0.0026	0.9924	1.71703 ± 0.112	2.39883 ± 0.15806	0.9450

Chemical and physical characterization of biochar and modified biochars

The values of pH, EC, composition of elements, atomic ratio, ash content, moisture content, specific surface area, total pores volume, and average pore diameter of BC and MBCs are shown in Table 2. These values are presented in this table as the mean of triplicate measurements ± standard deviation. Statistical analysis in Table 2 revealed highly significant differences ($p < 0.01$) among HBC, PBC, SBC, and BC for most measured chemical and physical properties, significant differences ($p < 0.05$) for EC (ms/cm) and total pores volume (cc/g), while insignificant differences among the biochars were observed for C % [$F(3,8) = 0.64$, $p = 0.613$] and moisture content % [$F(3,8 = 1.76$, $p = 0.233$]. This suggests that despite variations in preparation conditions, the fundamental carbonaceous structure and moisture content remained similar across all samples. Post-hoc analysis using Duncan's Multiple Range test indicated that most pairwise comparisons were statistically significant ($p < 0.05$). Different superscript letters within a row in Table 2 indicate significant differences according to Duncan's Multiple Range test at the $p < 0.05$ level of significance. A single superscript letter within a row indicates not significant difference.

The results in Table 2, show that the pH value decreased significantly ($p < 0.01$) in the case of MBCs compared to BC alone before modification that had an alkaline pH (Fakhar et al. 2025). These lower-pH MBCs can enhance the soil's cation exchange capacity, causing the soil to release essential alkaline cations (e.g. Ca^{2+} and Na^{+}) and instead adsorb more hydrogen (H^{+}) and aluminum (Al^{3+}) ions, which contributes to lowering soil pH and availability of essential nutrients such as phosphorus, iron, and zinc, which are often limited under high-pH conditions (Liu et al. 2025). Basic cations, which undergo pyrolysis to form oxides, hydroxides, and carbonates, as well as high electrical conductivity (EC), which suggests the existence of soluble salts, are typically responsible for the alkaline nature of BC. HBC had the lowest salinity in this investigation, whereas BC had the greatest salinity (as EC).

From Table 2, the carbon content and hydrogen content in the MBCs decreased, while nitrogen content and oxygen content increased. The increase in oxygen content and the decrease in carbon content after acid modification might be the result of acid treatment, where unsaturated carbon on BC surfaces is oxidized by H^{+} ions, strengthening oxygen-containing functional groups, which raise the oxygen content. At the same time, decarbonization gases such as CO_2 and CO are released, causing a relative decline in carbon content (Fu et al. 2025).

The H/C and O/C atomic ratios were calculated to evaluate the aromaticity and hydrophilicity of the particles, respectively. An increase in the O/C ratio indicates the finding of more oxygen-containing functional groups, while the decline in the H/C ratio suggests a rise in aromatic character, which may improve stability and utility of the MBCs (Ippolito et al. 2020). Clearly, the activation of BC by acids does not inhibit the decomposition of organic fractions. No significant differences in moisture content were found among all BC and MBCs. All BC and MBCs contained a small amount of moisture content (4.34-4.51%), which is consistent with the data in the available references. While the slight rise in ash content after acid modification (from 5.45 to 5.82%) may be the consequence of the development of new insoluble inorganic phases, as acid-derived anions can react with metal ions in the BC matrix, consistent with observations reported by Wang et al. (2022). However, these results indicate that the ash content of BC and MBCs fell within the medium range (5-10%wt), agreeing with Xiu et al. (2017).

The results in Table 2 also show that activation of BC by acids provided high specific surface area and total pores volume. Most of which are composed of micropores except BC is composed of mesopores. The average pore diameter of all MBCs materials was typical for microporous materials (< 2nm), while the average pore diameter of BC was characteristic of mesoporous materials (2-50 nm) (Marzeddu et al. 2022). The HA significantly ($p < 0.01$) improved the surface area of BC compared to sulfuric and phosphoric acids by adding active functional groups (e.g., -COOH and -OH), increasing microporosity, and dissolving carbon agglomerates, enhancing its ability for absorption and nutrient exchange. Therefore, these physicochemical improvements suggest that the MBCs, particularly HBC, could potentially ameliorate alkaline soil conditions and enhance nutrient availability for plant growth (Lan et al. 2024).

XRD analysis of biochar and modified biochars

Figure 3 explains the XRD spectra of BC and MBCs crystalline phase patterns. The result showed that BC patterns have some degree of crystallinity, particularly at specific angles (around 22° and 43°, corresponding to the (101) and (002) planes, respectively (Liu et al. 2020a)), indicating a partially ordered structure. These peaks were matched with ICDD standard cards (PDF-00-041-1487 for hexagonal graphite and PDF-01-073-5918 for rhombohedral graphite), confirming the crystalline phases. While the degree of crystallization of SBC patterns decreased a little.

Table 2. Characteristic of the biochar and modified biochars. Values are presented as mean ± standard deviation (n=3)

Characteristic	BC	MBCs			F (3,8)	p-value	sig
		PBC	SBC	HBC			
pH†	8.32±0.03^{a}	7.87±0.02^{b}	7.58±0.01^{c}	7.13±0.02^{d}	1666.89	<0.01	**
EC‡ (ms / cm)	0.22±0.01^{a}	0.21±0.01^{ab}	0.20±0.01^{ab}	0.19±0.01^{b}	5.00	0.031	*
Carbon (%)	67.92±2.32^{a}	65.78±1.82^{a}	65.82±3.06^{a}	67.07±1.52^{a}	0.64	0.613	ns
Hydrogen (%)	3.84±0.02^{a}	3.66±0.04^{b}	3.68±0.03^{b}	3.13±0.06^{c}	141.47	<0.01	**
Nitrogen (%)	1.81±0.04^{a}	1.97±0.01^{b}	2.13±0.00^{c}	2.52±0.02^{d}	529.67	<0.01	**
Sulfur (%)	0.05±0.00^{c}	0.04±0.01^{c}	1.21±0.14^{a}	0.81±0.13^{b}	110.52	<0.01	**
Ash content (%)	5.45±0.04^{c}	5.67±0.03^{b}	5.73±0.08^{b}	5.82±0.06^{b}	23.83	<0.01	**
Oxygen (%) “by difference”	20.93±0.08^{c}	22.88±0.02^{a}	21.43±0.06^{b}	20.65±0.02^{c}	1141.87	<0.01	**
Hydrogen / Carbon (H / C)	0.057±0.002^{a}	0.056±0.001^{a}	0.056±0.001^{a}	0.047±0.001^{b}	37.71	<0.01	**
Oxygen / Carbon (O / C)	0.31±0.02^{b}	0.35±0.01^{a}	0.33±0.02^{ab}	0.31±0.01^{b}	9.98	0.004	*
Moisture content (%)	4.34±0.09^{a}	4.41±0.07^{a}	4.45±0.07^{a}	4.51±0.13^{a}	1.76	0.233	ns
BET surface area (m² / g)	73.41±2.32^{c}	75.23±3.08^{bc}	79.60±2.14^{ab}	83.73±2.69^{a}	11.90	0.003	**
Total pores volume (cc / g)	0.05±0.00^{b}	0.06±0.00^{ab}	0.07±0.01^{a}	0.07±0.01^{a}	5.50	0.024	*
Average pore diameter (nm)	3.72±0.05^{c}	1.86±0.04^{ab}	1.83±0.02^{a}	1.92±0.03^{b}	1904.50	<0.01	**

Note: † Measured in BC / H_2O slurry at a 1:20 (w/v) ratio after stirring for 30 min. ‡ Measured in BC / H_2O slurry at a 1:10 (w/v) ratio at 25°C. BET surface area measured by N_2 adsorption at 77 K using the BET method. Pore size distribution calculated by BJH method. Different superscript letters within a row indicate significant differences according to Duncan’s Multiple Range test at the $p < 0.05$ level of significance. A single superscript letter within a row indicates the not significant difference. ** ($p < 0.01$), * ($p < 0.05$), and ns indicates not significant difference ($p \geq 0.05$)

The PBC patterns showed a more amorphous structure compared to BC and SBC patterns, where PBC may have disrupted the crystalline order in BC. The HBC patterns displayed the broadest and least defined peaks, indicating a highly amorphous structure. This amorphous nature enhances the number of reactive sites available for ion exchange and adsorption processes (Elbana et al. 2025). Hence, the results indicated that acid modification resulted in noticeable changes in peak intensity, indicating partial removal or transformation of mineral phases, and the greatest decrease was for HBC. Consequently, this decreasing enhances its ability to retain water and nutrients in the soil, making them more available to plants (Zhu et al. 2023). The crystallite size of BC and MBCs particles obtained from the Debye-Scherrer equation was on the nanoscale.

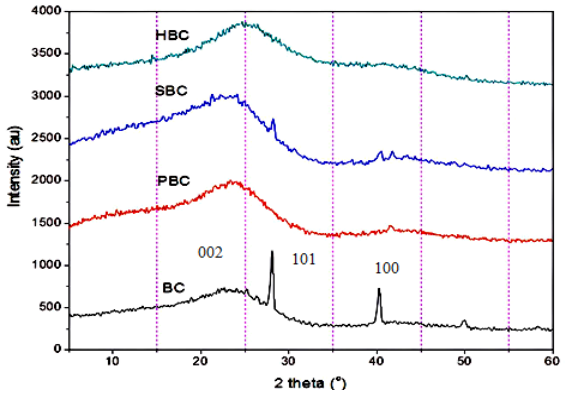

Figure 3. XRD patterns of BC and MBCs (PBC, SBC, and HBC). The major crystalline peaks correspond to 101, 100, and minor mineral components

FTIR spectra of biochar and modified biochars

Utilizing FTIR analysis (wavenumber range of 4000-450 cm^{-1}), the functional groups of BC and other MBCs (HBC, PBC, and SBC) were examined. Figure 4 shows numerous bioactive carbons with comparable infrared peaks but varying strengths. There were many peaks attributed to the stretching vibration of -CH_2 and -CH_3 in aliphatic hydrocarbons, as well as a large peak at 2950-3650 cm^{-1} associated with the stretching vibration of functional groups phenolic/carboxylic OH and C=O groups in -COOH (Ippolito et al. 2020; Swelam et al. 2020). The aliphatic -CH was represented by the peaks at 2862 cm^{-1} and 2921 cm^{-1} (Suriano et al. 2024). -COOH and C=O were represented by the peak at 1700 cm^{-1} (Mohammed et al. 2023).

A few reasonably stable aromatic compounds were progressively produced, as evidenced by the peak at 1610 cm^{-1}, which represented aromatic C=C. Phenolic C-OH was indicated by the peaks at 1187 cm^{-1} and 1260 cm^{-1} (El-Sayed et al. 2021). A trace amount of Si material in the biomass from dust or soil residuals created the peak at 1060 cm^{-1}, which displayed Si-O-Si (Liu et al. 2020b). The aromatic CH was shown by the peaks at 975 cm^{-1}, 836 cm^{-1}, and 795 cm^{-1} (Nandiyanto et al. 2022). FT-IR analysis revealed that the surfaces of BC and MBC were abundant in oxygen-containing functional groups, such as -OH, -C=O, and -COOH, indicating enhanced surface reactivity. In addition, hydroxyl and carboxyl groups are represented by relatively broad and deep peaks in HBC compared to PBC and SBC. This indicates that HBC possesses more function groups that contribute to the enhanced characteristics of BC. These functional groups increase cation-exchange capacity and proton donation ability, which can neutralize excessive alkalinity and improve nutrient availability in alkaline soils (Howe et al. 2024).

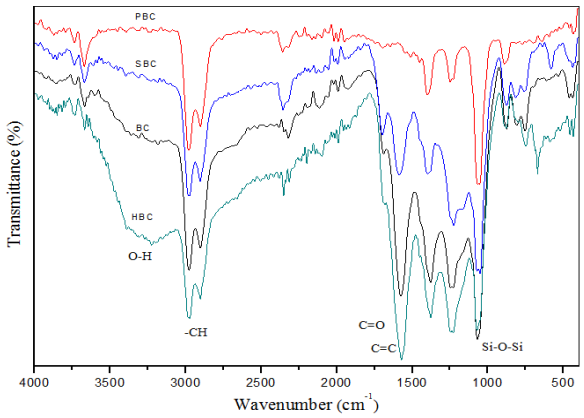

Figure 4. FTIR spectra of BC and MBCs (PBC, SBC, and HBC)

SEM analysis of biochar and modified biochars

To show how the surface modification changed the structure, SEM images of BC were taken before and after modification at different magnifications (1000× and 4000×) (Figure 5). The porosity and surface structure of materials influence their ability to absorb or interact with surrounding substances. This is crucial for applications in soil treatment and enhancement, especially for improving the condition of alkaline soils. The SEM image in Figure 5.A shows that BC has a porous surface structure with interconnected channels, which likely resulted from the release of volatile compounds during pyrolysis (Tiwari et al. 2022). This porous morphology provides a high surface area and abundant active sites that can enhance the adsorption and retention of water and nutrients, thereby contributing to the amelioration of alkaline soils (Elbana et al. 2025). When comparing SEM images taken before (Figure 5.A) and after (Figures 5.B-D), it was found that the elimination of contaminants had given the MBCs a more developed microporous structure (Yuan et al. 2020). The strong mineral acids (H_2SO_4 and H_3PO_4) produced highly ordered, honeycomb-like etching patterns (Figures 5. B and C). This distinct morphology is a direct visual confirmation of the aggressive and selective chemical attack that leads to the creation of a porous nanostructure.

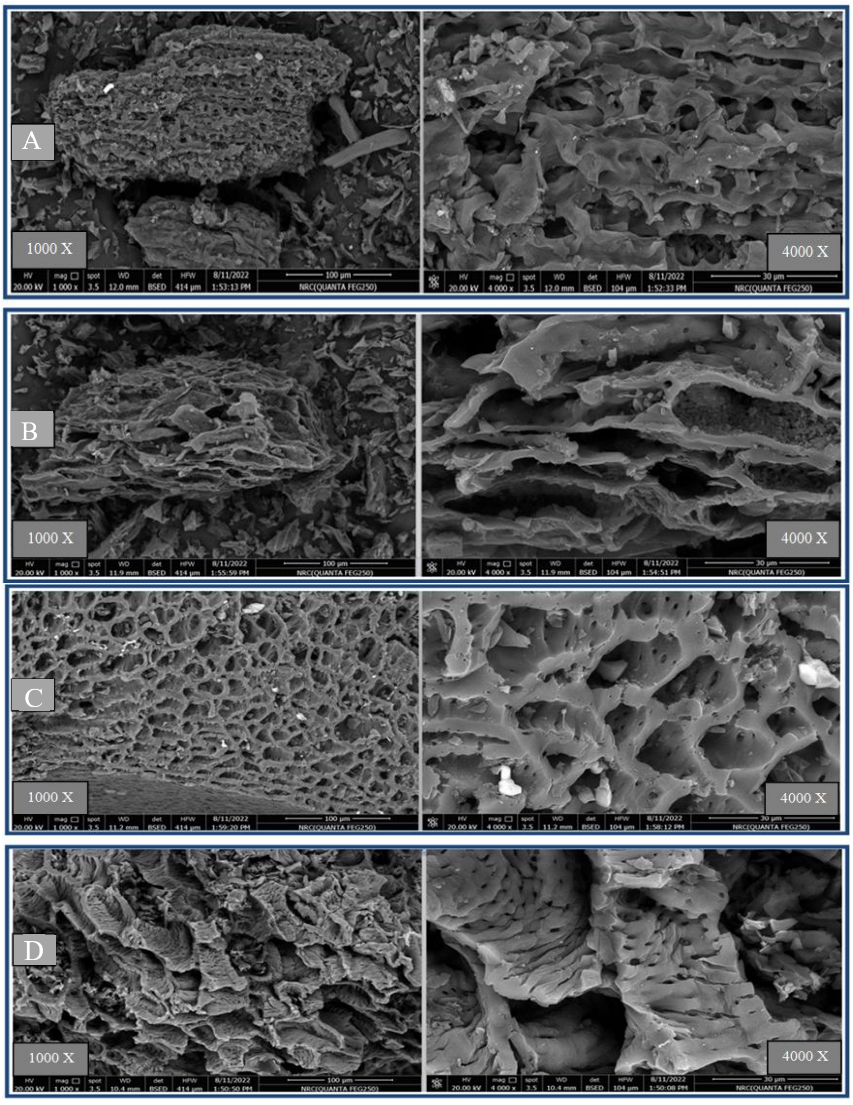

Figure 5. SEM images of A. BC, B. PBC, C. SBC, and D. HBC at two magnifications (1000× and 4000×)

These findings corroborate the BET results, which showed the higher specific surface area for SBC and PBC than BC, as the etched nanopores significantly increase the available surface area. Interestingly, the HBC yielded a qualitatively different morphology, characterized by a predominantly surface roughness interspersed with narrow, slit-like pores (Figure 5.D). This unique structure, combined with the BET results which showed a slightly higher specific surface area for the HBC compared to the SBC and PBC, suggesting a highly efficient modification pathway. In generally, the SEM images in Figure 5 indicated that BC and MBCs could be applied alkaline agricultural soils. Depending on their specific properties, such materials can improve water retention, nutrient availability, and overall soil health (Gong et al. 2024). SEM pictures showed that MBCs have a rougher, more porous surface than BC, which improves their active surface area, their capacity to retain water and nutrients, and facilitate their progressive release for improved alkaline soil performance (Liu et al. 2025). Additionally, the porous structure promotes root growth and nutrient uptake by increasing aeration and microbial activity (Holz et al. 2024). Consequently, MBCs are more efficient and applicable than BC for improving water availability and promoting steady plant growth in alkaline soils.

In conclusion, this study revealed that acid modification significantly improved the specific physicochemical properties, particularly in surface area, functional groups, and pH adjustment - of BC made from corncobs following the order: HBC>SBC>PBC>BC, owing to their increased surface area, enriched functional groups, and decreasing pH. The specific surface area of all the MBCs increased (from 75.23 to 83.73 m^2/g), while their pH decreased (from 7.87 to 7.13) compared to unmodified BC (73.41 m^2/g and 8.32, respectively). The HA significantly improved the surface area of BC compared to sulfuric and phosphoric acids by adding active functional groups (e.g., -COOH and -OH) and increasing microporosity as evidenced by its maximum surface area (83.73 $m^2\ g^{-1}$) and lowest pH value (7.13). This could potentially improve properties of alkaline soil by decreasing soil alkalinity, creating a more favorable environment for plant growth, thereby enhancing crop productivity, increasing farmers' income, improving local food security, and reducing environmental pollution through lower chemical fertilizer use and decreased open-field burning of agricultural residues. Therefore, further studies are needed to validate the laboratory results through controlled incubation and field experiments to determine the agronomic effectiveness, determine optimal application rates, and evaluate long-term field performance in terms of soil health and crop productivity. However, this study provides fresh perspectives on the comprehensive systematic comparison of three different acid modifications applied to corn cob BC. It also explicitly links the physicochemical improvements that result from these acid modifications to their potential use as soil amendments for alkaline soils. Moreover, long-term carbon sequestration is a positive side effect that helps mitigate climate change.

REFERENCES

Alhawas MS, Rafique MI, Ahmad M, Al-Wabel MI, Usman ARA, Al-Swadi HA, Al-Farraj AS. 2023. Ball mill, humic acid, and rock phosphate-modified conocarpus biochar for efficient removal of heavy metals from contaminated water. Sustainability 15: 11474. https://doi.org/10.3390/su151411474.

Ashour M, Belal R. 2020. An economic study for the agricultural wastes recycling project in Siwa Oasis. Al-Azhar J Agric Res 45 (2): 138-149. https://doi.org/10.21608/ajar.2020.150776.

Assirey EA, Altamimi LR. 2021. Chemical analysis of corn cob-based biochar and its role as water decontaminants. J Taibah Univers Sci 15 (1): 111-121. https://doi.org/10.1080/16583655.2021.1876350.

Bai Y, Ma R, Jing Z, Wan X, Tong J, Huang W, Liu J. 2024. Synthesis of Zn/Al layered double hydroxides magnetic-nanoparticle for removal of humic acid. Desalin Water Treat 317: 100097. https://doi.org/10.1016/j.dwt.2024.100097.

Dechapanya W, Khamwichit A. 2023. Biosorption of aqueous Pb (II) by H_3PO_4-activated biochar prepared from Palm Kernel Shells (PKS). Heliyon 9 (7): e17250. https://doi.org/10.1016/j.heliyon.2023.e17250.

Elbana TA, Bakr N, Shahin SA, Azab NAA, El-Ashry SM. 2025. Influence of acidified-biochar on phosphorus and potassium availability in alkaline sandy soil. Sci Rep 15 (1): 30504. https://doi.org/10.1038/s41598-025-16247-3.

Elkony A, Ibrahim A, El-Farah MA, Abd-Elhai F. 2020. Synthesis and characterization of (AAm-co-AHPS)/MMT hydrogel composites for the efficient capture of methylene blue from aqueous solution. Al-Azhar Bull Sci 31 (2): 31-46. https://doi.org/10.21608/absb.2020.39315.1079.

El-Naggar A, Lee SS, Rinklebe J, Farooq M, Song H, Sarmah AK, Ok YS. 2019. Biochar application to low fertility soils: A review of current status, and future prospects. Geoderma 337: 536-554. https://doi.org/10.1016/j.geoderma.2018.09.034.

El-Sayed MEA, Ahmed AF, Farghaly O, Abd-Elraheem MA, Elnasr TAS, Hassan MAM. 2018. Preparation and using modified nanohydroxyapatite molecules for wastewater treatment. Water Conserv Sci Eng 3 (4): 331-337. https://doi.org/10.1007/s41101-018-0061-7.

El-Sayed MEA, Hazman M, El-Rady AGA, Almas L, McFarland M, Din ASE, Burian S. 2021. Biochar reduces the adverse effect of saline water on soil properties and wheat production profitability. Agriculture 11 (11): 1112. https://doi.org/10.3390/agriculture11111112.

Fakhar A, Canatoy RC, Galgo S, Jane C, Rafique M, Sarfraz R. 2025. Advancements in modified biochar production techniques and soil application: A critical review. Fuel 400: 135745. https://doi.org/10.1016/j.fuel.2025.135745.

Fu M, Ma Y, Yang F, Xiao Z, Wang M, Bai S, Zhang Q, Liu H, Xu D, Zhang Y. 2025. Acid-modified biochar derived from agricultural waste for efficiently capturing low-concentration nitrous oxide (N_2O): Mechanisms and environmental implications. Toxics 13 (8): 623. https://doi.org/10.3390/toxics13080623.

Gong Y, Dan Y, Wang H, Gao W, Miao J, Sang W, Yuan H, Zheng S, Mohamed EAES, Islam AA, Zhang Y. 2024. Combined effect of leaching process and biochar application on the restoration of a coastal mild saline-alkali soil and the growth of pak choi (*Brassica chinensis* L.). Water Air Soil Pollut 235: 617. https://doi.org/10.1007/s11270-024-07433-6.

Hammam AA, Mohamed ES. 2020. Mapping soil salinity in the East Nile Delta using several methodological approaches of salinity assessment. Egypt J Remote Sens Space Sci 23: 125-131. https://doi.org/10.1016/j.ejrs.2018.11.002.

Hammerschmiedt T, Holatko J, Pecina V, Huska D, Latal O, Kintl A, Muhammad S, Gusiatin ZM, Kolackova M, Nasir M, Baltazar T, Ahmed N, Brtnicky M. 2021. Assessing the potential of biochar aged by humic substances to enhance plant growth and soil biological activity. Chem Biol Technol Agric 8: 46. https://doi.org/10.1186/s40538-021-00242-7.

Holz M, Zarebanadkouki M, Benard P, Hoffmann M, Dubbert M. 2024. Root and rhizosphere traits for enhanced water and nutrients uptake efficiency in dynamic environments. Front Plant Sci 15: 1383373. https://doi.org/10.3389/fpls.2024.1383373.

Howe JA, McDonald MD, Burke J, Robertson I, Coker H, Gentry TJ, Lewis KL. 2024. Influence of fertilizer and manure inputs on soil

health: A review. Soil Secur 16: 100155. https://doi.org/10.1016/j.soisec.2024.100155.

Ippolito JA, Cui L, Kammann C, Wrage-Mönnig N, Estavillo JM, Fuertes-Mendizabal T, Cayuela ML, Sigua G, Novak J, Spokas K, Borchard N. 2020. Feedstock choice, pyrolysis temperature and type influence biochar characteristics: A comprehensive meta-data analysis review. Biochar 2 (4): 421-438. https://doi.org/10.1007/s42773-020-00067-x.

Joshi M, Bhatt D, Srivastava A. 2023. Enhanced adsorption efficiency through biochar modification: A comprehensive review. Ind Eng Chem Res 62 (35): 13748-13761. https://dx.doi.org/10.1021/acs.iecr.3c02368.

Jubori HK, Kaynak AB. 2025. The impact of climate change on water diplomacy in the Middle East. Intl J Adv Humanit Res 5 (2): 1-21. https://doi.org/10.21608/ijahr.2025.386408.1067.

Kopp C, Regueiro I, Stoumann-Jensen L, Müller-Stöver D, Fangueiro D. 2024. Enhancing phosphorus availability in biochar: Comparing sulfuric acid treatment to biological acidification approaches. J Plant Nutr Soil Sci 187 (4): 737-747. https://dx.doi.org/10.1002/jpln.202300404.

Lan W, Zhao X, Wang Y, Jin X, Ji J, Cheng Z, Yang G, Li H, Chen G. 2024. Research progress of biochar modification technology and its application in environmental remediation. Biomass Bioenergy 184: 107178. https://doi.org/10.1016/j.biombioe.2024.107178.

Liu C, Wang W, Wu R, Liu Y, Lin X, Kan H, Zheng Y. 2020b. Preparation of acid- and alkali-modified biochar for removal of methylene blue pigment. ACS Omega 5 (48): 30906-30922. https://doi.org/10.1021/acsomega.0c03688.

Liu P, Ptacek CJ, Blowes DW, Finfrock YZ, Liu Y. 2020a. Characterization of chromium species and distribution during Cr (VI) removal by biochar using confocal micro-X-ray fluorescence redox mapping and X-ray absorption spectroscopy. Environ Intl 134: 105216. https://doi.org/10.1016/j.envint.2019.105216.

Liu S, Cen B, Yu Z, Qiu R, Gao T, Long X. 2025. The key role of biochar in amending acidic soil: Reducing soil acidity and improving soil acid buffering capacity. Biochar 7: 52. https://doi.org/10.1007/s42773-025-00432-8.

Marzeddu S, Décima MA, Camilli L, Bracciale MP, Genova V, Paglia L, Marra F, Damizia M, Stoller M, Chiavola A, Boni MR. 2022. Physical-chemical characterization of different carbon-based sorbents for environmental applications. Materials 15 (20): 7162. https://doi.org/10.3390/ma15207162.

Mohammed E, Elsheikh MM, El-Zomrawy AA, Ahmed FA. 2023. Novel technique in production of PB (II)- imprinted polymers. Al-Azhar Bull Sci 34 (1): 52-63. https://doi.org/10.58675/2636-3305.1633.

Nandiyanto ABD, Ragadhita R, Fiandini M. 2022. Interpretation of Fourier Transform Infrared Spectra (FTIR): A practical approach in the Polymer/Plastic thermal decomposition. Indones J Sci Tech 8 (1): 113-126. https://doi.org/10.17509/ijost.v8i1.53297.

Otaibi FA, Alghamdi S, Abo-Elyousr K. 2024. The influence of salinity on plant growth and amendment strategies. Sohag J Sci 9 (3): 261-267. https://doi.org/10.21608/sjsci.2024.258471.1168.

Phares CA, Atiah KF, Kwame A, Danquah A, Asare AT, Aggor-Woananuc S. 2020. Application of biochar and inorganic phosphorus fertilizer influenced rhizosphere soil characteristics, nodule formation and phytoconstituents of cowpea grown on tropical soil. Heliyon 6 (10): e05255. https://doi.org/10.1016/j.heliyon.2020.e05255.

Reza MS, Afroze S, Bakar MSA, Saidur R, Aslfattahi N, Taweekun J, Azad AK. 2020. Biochar characterization of invasive *Pennisetum purpureum* grass: Effect pyrolysis temperature. Biochar 2 (2): 239-251. https://doi.org/10.1007/s42773-020-00048-0.

Suriano R, Magni M, Tagliabue B, Re V, Ciapponi R, Nasti R, Cavallaro M, Beretta G, Turri S, Levi M. 2024. Highly pure curing agent from tomato waste for bio-based anti-corrosion epoxy coatings. Eur Polym J 223: 113629. https://doi.org/10.1016/j.eurpolymj.2024.113629.

Swelam A, Gedamy Y, Elshahed A. 2020. Preparation of activated carbon from ion exchange resin waste and its application for manganese removal from groundwater. Al-Azhar Bull Sci 31 (1): 33-49. https://doi.org/10.21608/absb.2020.111469.

Swift RS. 1996. Organic matter characterization. In: Sparks DL, Bartels JM, Bigham JM (eds.). Methods of Soil Analysis: Part 3. Chemical Methods. Soil Science Society of America, Madison WI. https://doi.org/10.2136/sssabookser5.3.c35.

Tenic E, Ghogareh R, Dhingra A. 2020. Biochar - A panacea for agriculture or just carbon? Horticulturae 6 (3): 37. https://doi.org/10.3390/horticulturae6030037.

Tessema N, Yadeta D, Kebede A, Ayele GT. 2022. Soil and irrigation water salinity, and its consequences for agriculture in Ethiopia: A systematic review. Agriculture 13 (1): 109. https://doi.org/10.3390/agriculture13010109.

Tiwari SK, Bystrzejewski M, De Adhikari A, Huczko A, Wang N. 2022. Methods for the conversion of biomass waste into value-added carbon nanomaterials: Recent progress and applications. Prog Energy Combust Sci 92: 101023. https://doi.org/10.1016/j.pecs.2022.101023.

Tomczyk A, Sokołowska Z, Boguta P. 2020. Biochar physicochemical properties: Pyrolysis temperature and feedstock kind effects. Rev Environ Sci Biotechnol 19: 191-215. https://doi.org/10.1007/s11157-020-09523-3.

Wang H, Sheng L, Zang S. 2023. Study on H_2SO_4-modified corn straw biochar as substrate material of constructed wetland. Environ Sci Pollut Res 30 (54): 115556-115570. https://doi.org/10.1007/s11356-023-30569-7.

Wang X, Sun T, Ma H, Tang G, Chen M, Abulaizi M, Yu G, Jia H. 2022. Effects of acidic phosphorus-rich biochar from halophyte species on P availability and fractions in alkaline soils. Chem Biol Technol Agric 9 (1): 101. https://doi.org/10.1186/s40538-022-00374-4.

Wu B, Yang H, Li S, Tao J. 2024. The effect of biochar on crop productivity and soil salinity and its dependence on experimental conditions in salt-affected soils: A meta-analysis. Carbon Res 3 (1): 56. https://doi.org/10.1007/s44246-024-00138-9.

Xiu S, Shahbazi A, Li R. 2017. Characterization, modification and application of biochar for energy storage and catalysis: A review. Trend Renew Energy 3: 86-101. https://dx.doi.org/10.17737/tre.2017.3.1.0033.

Yuan S, Hong M, Li H, Ye Z, Gong H, Zhang J, Huang Q, Tan Z. 2020. Contributions and mechanisms of components in modified biochar to adsorb cadmium in aqueous solution. Sci Total Environ 733: 139320. https://doi.org/10.1016/j.scitotenv.2020.139320.

Yuanbo S, Jiawei T, Mengyu J, Zhe L, Jianfei Z, Mohamed EAE, Islam AA, Yalei Z, Zheng S. 2025. Effect of pyrolysis temperature and heating rate on the physicochemical properties of alkali lignin-derived biochar: A comparative study of fast and slow pyrolysis. J Anal Appl Pyrolysis 191: 107236. https://dx.doi.org/10.1016/j.jaap.2025.107236.

Zhang X, Zuo Y, Wang T, Han Q. 2024. Salinity effects on soil structure and hydraulic properties: Implications for pedotransfer functions in coastal areas. Land 13 (12): 2077. https://doi.org/10.3390/land13122077.

Zhu S, Liu J, Tang G, Sun T, Jia H, Zhao H, Zhang Y, Lin L, Xu W. 2023. Evaluating the application potential of acid-modified cotton straw biochars in alkaline soils based on entropy weight TOPSIS. Agronomy 13 (11): 2807. https://doi.org/10.3390/agronomy13112807.